

## Rapid Report

# Does the formation of the $S_3$ -state in $Ca^{2+}$ -depleted Photosystem II correspond to an oxidation of Tyrosine Z detectable by cw-EPR at room temperature?

Alain Boussac<sup>\*</sup>, A. William Rutherford

*SBE, DBCM, URA CNRS 1290, CEA Saclay, 91191 Gif sur Yvette Cedex, France*

Received 31 March 1995; accepted 5 April 1995

## Abstract

The tyrosine EPR signal(s) have been investigated at room temperature in  $Ca^{2+}$ -depleted Photosystem II. It was found that at low, non-saturating microwave powers, the tyrosine signal present after flash illumination decayed monophasically in about 40% of the centers with a  $t_{1/2}$  of 780 s. This decay is attributed to  $TyrD^\circ$  reduction. The radical formed as the formal  $S_3$  state and detected as a split EPR signal at helium temperature, decayed monophasically at room temperature with a  $t_{1/2}$  of 110 s. When the tyrosine EPR signals were monitored at room temperature using a high, saturating microwave power, in addition to the 780 s phase, a faster phase of 110 s was observed. This additional phase is attributed to  $TyrD^\circ$ , the amplitude of which is enhanced by dipolar coupling to the fast relaxing  $S_3$  state. Its decay corresponds to the loss of the fast relaxing  $S_3$  species. Similar effects reported earlier and attributed to the formation of  $TyrZ^\circ$  are reinterpreted as a relaxation enhancement of  $TyrD^\circ$ . No evidence was found from this approach to attribute the split  $S_3$  EPR signal to a  $TyrZ^\circ$  signal which is detectable at room temperature.

**Keywords:** EPR; Free radical; Microwave saturation; Oxygen evolution

Photosystem II catalyses light-driven water oxidation resulting in oxygen evolution. Absorption of a photon leads to a charge separation between a chlorophyll molecule, designated P680, and a pheophytin molecule. The pheophytin anion transfers the electron to a quinone,  $Q_A$ , and  $P680^+$  is reduced by a tyrosine residue,  $TyrZ$ , the tyrosine-161 of the D1 polypeptide [1–6]. A cluster of 4 Mn located in the reaction center of PS II probably acts both as the active site and as a charge-accumulating device of the water-splitting enzyme [1–6]. During the enzyme cycle, the oxidizing side of PS II goes through five different redox states that are denoted  $S_n$ ,  $n$  varying from 0 to 4 [7]. The oxygen is released during the  $S_3$  to  $S_0$  transition, in which  $S_4$  is a transient state. In addition to  $TyrZ$ , there

is a second redox-active tyrosine in PS II,  $TyrD$ , the tyrosine-160 of the D2 polypeptide [8,9], the radical of which is normally more stable in the dark [5,6,8,9].

$Ca^{2+}$  and  $Cl^-$  are two essential cofactors for oxygen evolution [10–12]. In  $Ca^{2+}$ -depleted and  $Cl^-$ -depleted PS II, inhibition of the enzyme cycle occurs at the  $S_3$  to  $S_0$  transition [13,14].  $Ca^{2+}$  removal is achieved by salt-washing the membranes in the light. The addition, in the light, of a range of chelators (EGTA, EDTA, citrate, pyrophosphate, etc.) during or after the salt-washing procedure in the light, results in an additional modification of the enzyme manifest as a major modification of the spectral properties of the  $S_2$ -multiline and also as the stabilization of the  $S_2$ -multiline signal [15,16].

Continuous or flash illumination of  $Ca^{2+}$ -depleted PS II induced the formation of the split  $S_3$  EPR signal centered at  $g = 2$  with a width of 164 G [15,17]. The appearance of the split  $S_3$  EPR signal is accompanied by the disappearance of the multiline signal in cw-EPR [15,17] but not by the disappearance of the  $S_2$  manganese signal as detected by field swept spectra using pulsed EPR [18]. These results were explained by a magnetic interaction between the

Abbreviations: P680, reaction center chlorophyll (Chl) of Photosystem II (PS II);  $TyrZ$ , the tyrosine acting as the electron donor to P680;  $TyrD$ , the tyrosine acting as a side-path electron donor of PS II;  $Q_A$ , primary quinone electron acceptor of PS II; Mes, 2-(*N*-morpholino)ethanesulfonic acid; PPBQ, phenyl-*p*-benzoquinone.

<sup>\*</sup> Corresponding author. Fax: +33 1 69088717.

Mn-cluster and an organic free radical formed in the  $S_2$  to  $S_3$  transition [15,17,18]. Originally,  $\text{TyrZ}^\circ$  was not seriously considered as a candidate because, according to earlier literature results [13,19,20],  $\text{TyrZ}^\circ$  seemed to be light-induced after the  $S_3$  state was formed in  $\text{Ca}^{2+}$ -depleted PS II. These results were subsequently reinterpreted on the basis of new data showing the lack of  $\text{TyrZ}^\circ$  formation under these conditions [21]. This opened the door for  $\text{TyrZ}^\circ$  to play the role as organic radical interacting with the Mn cluster. The origin of the split EPR signal, i.e., His versus Tyr, has been discussed in detail elsewhere [5,22–24]. From its UV-visible and FTIR spectra, the radical was suggested to be a histidine radical [17,25]. However, the report of an abnormally long-lived  $\text{Tyr}^\circ$  signal attributed to  $\text{TyrZ}^\circ$ , in the presence of the split EPR signal, complicated the picture [26]. This, however, was shown to be based on erroneous interpretations of data [27]. Nevertheless, similar observations have been made now in a number of laboratories ([28,29] plus several others as evidenced by discussion in recent conferences). What has been reported is the detection at room temperature of a light-induced and abnormally slow-decaying  $\text{Tyr}^\circ$  EPR signal under conditions in which the split EPR signal is formed. This implies that at low temperature  $\text{TyrZ}^\circ$  would be magnetically coupled to the Mn-cluster (resulting in a split EPR signal) and that at room temperature  $\text{TyrZ}^\circ$  would be observed as a free radical. Due to the difficulty in detecting the  $\text{Tyr}^\circ$  EPR signals at room temperature with a low microwave power, the experiments reporting an increase in the  $\text{Tyr}^\circ$  EPR signal were done with high microwave powers. It was shown earlier that formation of  $S_3$  resulted in a saturation enhancement of the  $\text{TyrD}^\circ$  signal as measured at 50 K [27]. Similar results were found at room temperature in the presence of a high concentrations of ferricyanide and ferrocyanide [25]. In this work, we have investigated the behavior at room temperature of the  $\text{Tyr}^\circ$  EPR signals at different microwave powers and after different dark periods following flash illumination. The stability at room temperature of the  $\text{Tyr}^\circ$  EPR signals has been compared to that of the species giving rise to the split EPR signal detected at low temperature. The denomination ' $\text{Tyr}^\circ$  signal' is used as a generic term when no distinction between the species from which it originates, i.e.,  $\text{TyrD}^\circ$  or  $\text{TyrZ}^\circ$ , is made. The denomination 'split EPR signal' is also used to characterize the species from which it originates. Although this signal is measured at 10 K, the stability of the split EPR signal refers to the stability at room temperature of the species from which it originates.

Calcium-depleted, EGTA-treated and polypeptide-reconstituted Photosystem II membranes were prepared as previously described [15]. All the experiments were carried out in a medium containing 0.3 M sucrose, 25 mM Mes (pH 6.5) and 10 mM NaCl.

CW-EPR data were recorded at liquid helium temperatures or at room temperature with a Bruker ESR 300e or a

Bruker ER200D spectrometers at X-band equipped with an Oxford Instruments cryostat for low-temperature measurements. For low-temperature measurements, the PS II membranes were put in calibrated quartz EPR tubes and, after dark adaptation, 1 mM PPBQ (dissolved in dimethyl sulfoxide) was added as an artificial electron acceptor. The samples were illuminated at room temperature and further dark-adapted at room temperature as indicated, then frozen at 200 K in a  $\text{CO}_2$ /ethanol bath and transferred to 77 K. For room-temperature measurements the samples were put in a quartz flat cell with 1 mM PPBQ and illuminated directly in the EPR cavity. Flash illuminations were done with a Nd-YAG laser (330 mJ, 15 ns, Quantel). Flash illumination was saturating for 3 mg/ml of Chl, but the concentration of the samples used in these experiments was 1–2 mg Chl/ml, except for the experiments reported in Figs. 1 and 6, for which the Chl concentration was 4 mg/ml.

In Fig. 3A, amplitude of the signals has been estimated by double integration of the spectra recorded at different microwave powers. The time required to record each spectrum was 10 s. Ten spectra were averaged. For the flash-illuminated samples and to complete the formation of the  $S_3$  state, ten flashes were given prior to the recording of the first spectrum. To maintain the sample in the  $S_3$  state, two flashes (spaced by 1 s) were given at the beginning of each scan. The  $\text{Tyr}^\circ$  signal was recorded in the dark immediately after the flash illumination (the peak of the signal was recorded 2–3 s after the last flash). This procedure was used instead of continuous illumination to avoid any contribution from the fraction of the  $\text{Tyr}^\circ$  signal, which decayed in the hundred millisecond time-range. The dark period of 2 s also corresponded to the time required to freeze the sample in experiments reported in Fig. 4.

The fitting procedure employed the 'GraFit' program Version 3.0, Erithacus Software, Staines, UK.

Fig. 1 shows low-temperature EPR spectra recorded with the PS II membranes used in this study. Spectrum (a) corresponds to the dark-adapted state. It exhibits the modified Mn multiline signal, between 2400 and 4200 G, characteristic of the stable  $S_2$ -state in the  $\text{Ca}^{2+}$ -depleted, EGTA-treated and polypeptide-reconstituted PS II [15]. Illumination at room temperature by ten flashes results in the characteristic split EPR signal (spectrum b) [15] with a peak to trough of 164 G and centered at  $g = 2$  (3350 G). This signal was previously attributed to the magnetic interaction of a radical with the Mn-cluster [15,17].

The amplitude of the  $\text{Tyr}^\circ$  signal was firstly recorded at room temperature with a high microwave power (200 mW). Measurements were done in dark-adapted samples during and after flash illumination. Effects of illumination by five flashes on a sample dark-adapted for 30 min in the EPR cavity are shown in Fig. 2. The five flashes induced an increase of the  $\text{Tyr}^\circ$  signal. Although the intensity of the laser flash was saturating, the light-induced signal reached its maximum only after the fifth flash. This is attributed to

the lower than normal quantum yield of  $S_3$  formation in  $Ca^{2+}$ -depleted PS II [17,21]. Only a small fraction of the light-induced  $Tyr^\circ$  signal decayed in the hundred millisecond time-range after each flash of the series. This fast decay arises from  $TyrZ^\circ$  formed in the small proportion of irreversibly inhibited centers [20]. The major part of the light-induced signal decayed slowly in the dark. The best fitting of the slow decay required a biphasic exponential process (18%,  $t_{1/2} = 780$  s; 82%,  $t_{1/2} = 110$  s, continuous line through the experimental points). The data cannot be fitted by a monophasic decay (Fig. 2, dashed line). If the fitting procedure was done using a monophasic exponential decay plus an offset, the agreement with the experimental curve improved but remained poorer than with a double exponential decay (in this case, the offset replaced the slow phase and the  $t_{1/2}$  increased to 190 s). In what follows, the fast phase of the  $Tyr^\circ$  decay will refer to the phase with a  $t_{1/2}$  of 110 s and the slow phase to that which decays with a  $t_{1/2}$  of 780 s.

Kinetic measurements done at room temperature, with a very low microwave power and at a single field position, are difficult due to the resulting poor signal-to-noise ratio. Instead, to circumvent the problem, spectra of the signals were recorded after different dark periods following the

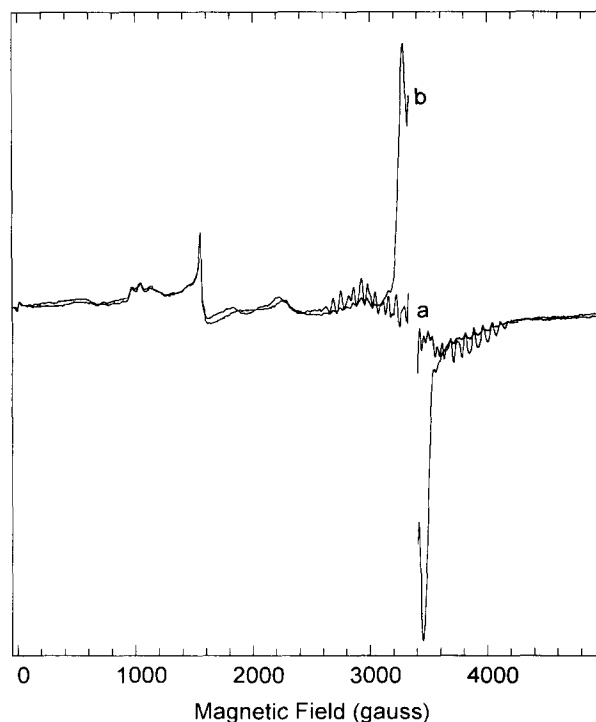


Fig. 1. EPR spectra of  $Ca^{2+}$ -depleted, EGTA-treated and polypeptide-reconstituted PS II. Spectrum a, dark-adapted membranes. Spectrum b, same sample as for spectrum a but after illumination by 20 flashes at room temperature. After the illumination, the sample was rapidly frozen at 200 K then at 77 K. Instrument settings: temperature, 10 K; modulation amplitude, 22 G; microwave power, 20 mW; microwave frequency, 9.4 GHz; modulation frequency, 100 kHz. The central parts of the spectra corresponding to the  $TyrD^\circ$  region were deleted.

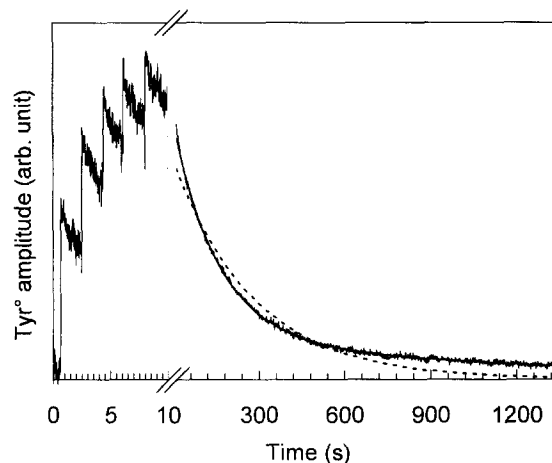


Fig. 2. Amplitude of the  $Tyr^\circ$  EPR signal induced by flash illumination and kinetics of the subsequent dark disappearance in  $Ca^{2+}$ -depleted, EGTA-treated and polypeptides-reconstituted PS II. Instrument settings: Room temperature (about 20°C); microwave frequency, 9.74 GHz; modulation amplitude, 4 G; time constant, 10 ms for the left part of the graph and 320 ms for the right part of the graph; microwave power 200 mW; chlorophyll concentration, 1.5 mg/mL. The traces were recorded at a magnetic field of 3462 G, i.e., the low field maximum of the  $Tyr^\circ$  signal (see Fig. 3). The continuous line in the right part of the graph corresponds to the fitting of the experimental data points obtained using a biphasic exponential decay. The dashed line was obtained using a mono exponential decay.

illumination. A similar protocol has already been used [25]. Fig. 3A shows the effect of the microwave power on the amplitude of the  $Tyr^\circ$  signal estimated by double integration. The light-induced signals (closed squares) were recorded after flash illumination, and the dark signals (open circles) were recorded after dark-adaptation for 5 min at room temperature. The light-induced signals were not recorded under continuous illumination to avoid any contribution from the  $Tyr^\circ$  signal decaying in the hundred millisecond time-range. The  $Tyr^\circ$  signal in dark-adapted samples is saturated at 200 mW and the  $Tyr^\circ$  signal recorded in the illuminated sample increased about 2.5-times. In non-saturating conditions, with a low microwave power (below 0.2 mW, i.e., 30 dB), the amplitude of the signal after 5 min of dark adaptation represents 77% of that of the signal recorded after flash illumination. Fig. 3B shows the dark spectrum (a) and the light-induced spectrum (b) recorded with a microwave power of 0.02 mW (40 dB).

The light-induced  $Tyr^\circ$  signal in saturating conditions can be explained in two different ways. First, it could arise from  $TyrZ^\circ$ , which decays with a  $t_{1/2}$  of 110 s at room temperature in  $Ca^{2+}$ -depleted PS II. Second, it could correspond to a saturation enhancement effect of  $TyrD^\circ$  due to the formation of  $S_3$  as already observed in this material at 50 K [27]. To discriminate between these two possibilities, we first monitored the stability at room temperature of the species giving rise to the split EPR signal. Then, this stability was compared to that of  $Tyr^\circ$  measured with a

high, saturating microwave power and with a low, non-saturating microwave power.

Samples were put in calibrated quartz EPR tubes at the same Chl concentration as that in Fig. 2 and were dark-adapted at room temperature, submitted to five flashes and further dark-adapted for various times before being frozen. Fig. 4A shows the split EPR signals after various dark-adaptation periods. The time-course of the amplitude of the spectra is plotted in Fig. 4B. The decay is monophasic, with a  $t_{1/2}$  equal to 120 s. The data cannot be fitted by a biphasic process. The comparisons between the different phases and experiments are illustrated in Fig. 5.

Fig. 5A shows the  $\text{Tyr}^\circ$  decay which was taken from Fig. 2 (curve a) and its decomposition into the fast phase (curve b) and slow phase (curve c). Curves d<sub>1</sub>, d<sub>2</sub> and d<sub>3</sub> represent the decay of the split EPR signal deduced from Fig. 4 and normalized to curves a, b and c at  $t = 0$ , respectively. Fig. 5A (open circles) also shows the amplitude of the  $\text{TyrD}^\circ$  signal measured at 10 K with a non-saturating microwave power in the same samples as those used for the measurement of the split EPR signal at 10 K

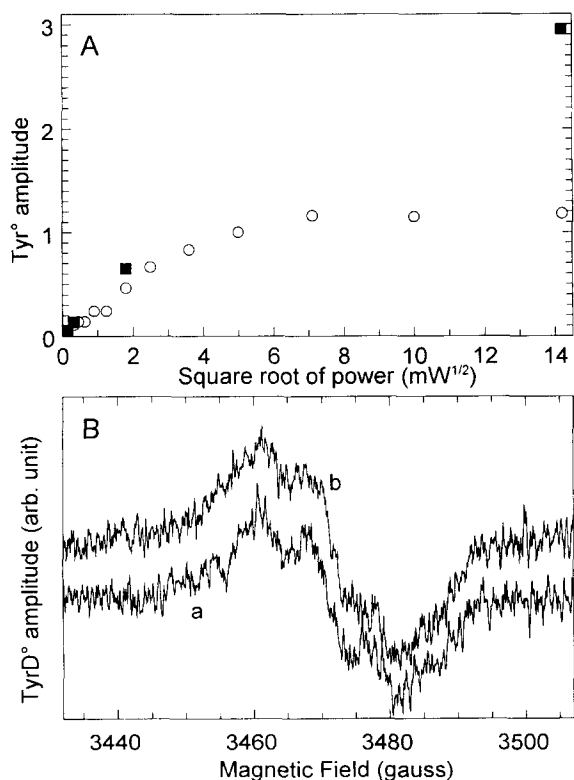


Fig. 3. (A) Microwave power saturation at room temperature of  $\text{Tyr}^\circ$  in  $\text{Ca}^{2+}$ -depleted, EGTA-treated and polypeptide-reconstituted PS II. Open circles,  $\text{TyrD}^\circ$  signal measured after a dark-adaptation for 5 minutes following illumination by 5 flashes; Closed squares, light-induced  $\text{Tyr}^\circ$  signal recorded 2–10 s after flash illumination. (B)  $\text{Tyr}^\circ$  EPR spectra. Spectra a and b correspond respectively to the dark-adapted and flash illuminated samples in which the  $\text{Tyr}^\circ$  signal was measured in panel A with a microwave power of 20  $\mu\text{W}$ . Instrument settings: modulation amplitude, 4 G; microwave frequency, 9.75 GHz; modulation frequency, 100 kHz.

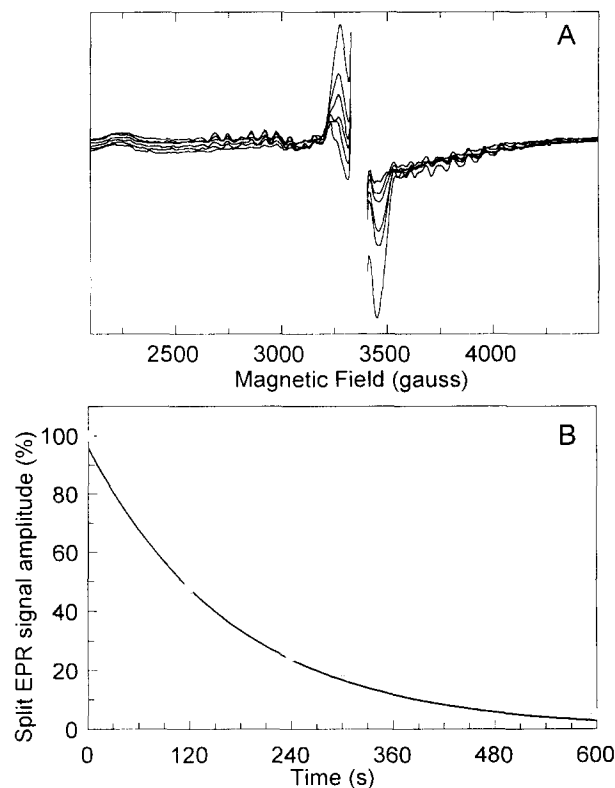


Fig. 4. (A) EPR spectra of PS II membranes illuminated by a series of five flashes spaced by 1 s and dark-adapted for various periods at room temperature. Same instrument settings as for Fig. 1. The dark periods prior freezing the samples were 0, 1, 2, 4, 5 and 10 min. The central parts of the spectra corresponding to the  $\text{TyrD}^\circ$  region were deleted. (B) Amplitude of the split EPR signals shown in panel A versus the time of the dark incubation at room temperature prior to the freezing of the samples. Each point was estimated by a computer interactive subtraction of the signal at  $t = 0$ . The continuous line drawn through the points corresponds to the best fit obtained with a mono exponential decay (see text).

(Fig. 4). In these conditions the  $\text{Tyr}^\circ$  signal observed as a free radical can arise only from  $\text{TyrD}^\circ$ , since the other radical is magnetically coupled to the Mn-complex (i.e., it is seen as the split signal). The closed triangles correspond to the amplitude of the two spectra shown in Fig. 3B. The amplitudes of  $\text{TyrD}^\circ$  at  $t = 0$  have been normalized to the amplitude of curve c at  $t = 0$ . Five observations can be made: (i) the kinetics of the split EPR signal is close (but see next paragraph) to the fast phase of the  $\text{Tyr}^\circ$  decay measured with a high microwave power; (ii) when the split EPR signal has disappeared, the  $\text{Tyr}^\circ$  signal continues to decay; (iii) the slow phase matches the decay of the  $\text{Tyr}^\circ$  signal measured with a low, non-saturating microwave power; (iv) the slow phase corresponds to the decay of  $\text{TyrD}^\circ$  in about 40% of the centers; (v) no contribution from kinetics with a  $t_{1/2}$  of 110 s (nor 190 s) seems to be present in the decay of  $\text{Tyr}^\circ$  at low microwave power.

When all the split EPR signal has disappeared, the  $\text{Tyr}^\circ$  decay corresponds to the  $\text{TyrD}^\circ$  reduction. By contrast, for the short times the  $\text{Tyr}^\circ$  decay measured in saturating

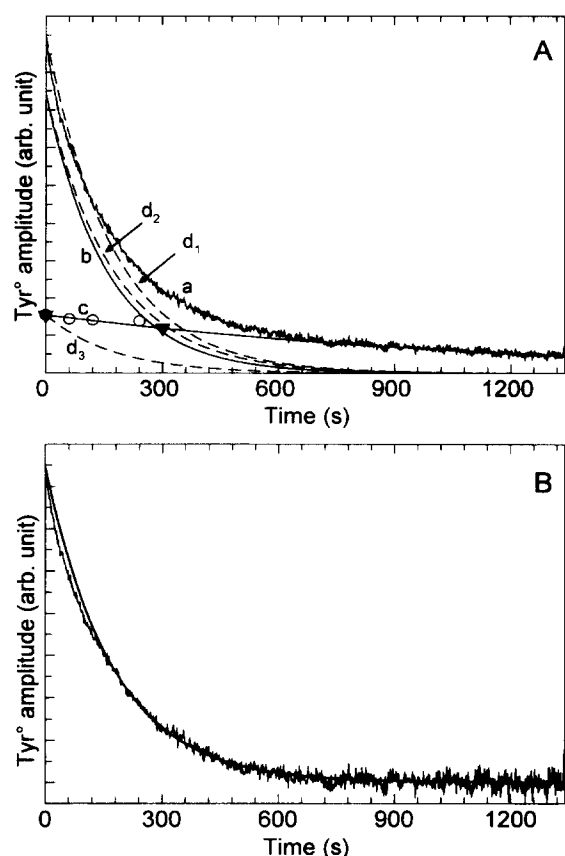


Fig. 5. (A) Curve a, same curve as in the right part of Fig. 2; curves b and c, fast and slow components of curve a; dashed curves  $d_1$ ,  $d_2$  and  $d_3$ , mono exponential decays with a  $t_{1/2}$  equal to 110 s and normalized at  $t = 0$  to curves a, b and c, respectively. Open circles, amplitude of TyrD° in the samples used in Fig. 4A measured at 10 K and with a microwave power of 1  $\mu$ W. Closed triangles, amplitude of the spectra in Fig. 3B. Amplitudes of TyrD° were normalized to curve c at  $t = 0$ . (B) The continuous line corresponds to a monoexponential decay with a  $t_{1/2}$  equal to 110 s, i.e., the decay of the split EPR signal measured at room temperature in Fig. 4. The other trace was obtained as indicated in the text and corresponds to the decay of the split EPR signal at room temperature deduced from Fig. 2.

conditions should be in fact described by the following equation:

$$\text{Tyr}_t^\circ = \text{Tyr}_{t=0}^\circ * \exp(-((\ln 2)/110) * t) \propto K \times \exp(-(k_{\text{split}} + k_D) * t) \quad (1)$$

in which  $k_D$  and  $k_{\text{split}}$  are the rate constants of the reduction of TyrD° and of the split EPR signal in the dark, respectively.  $K$  is the saturation enhancement factor of TyrD° induced by the formation of the split EPR signal ( $K = \text{Tyr}_{t=0}^\circ / \text{Tyr}_{t=0}^\circ$ ). Since the data show that TyrD° is reduced with the same kinetics in the presence as in the absence of the split EPR signal (i.e.,  $k_D = (\ln 2)/780$ ), the decay of the split EPR signal (i.e., the term  $\exp(-k_{\text{split}} \cdot t)$ ) can be deduced from Eq. (1). Fig. 5B compares this decay

to the decay of the split EPR signal directly measured in Fig. 4. Both curves are normalized to the same amplitude at  $t = 0$  and match very well.

All the results presented above can be explained by assuming that the increase in the TyrD° signal at high microwave powers originates from: (i) a relaxation enhancement of TyrD° due its magnetic interaction with a light-induced faster relaxing species [25,27]; (ii) TyrD° which decays with a  $t_{1/2}$  equal to 780 s in a fraction of the centers. When the microwave power is low enough to avoid saturation of TyrD°, no decay of the TyrD° signal corresponding to that of the split EPR signal was found. In these conditions, the TyrD° decay corresponds to the TyrD° decay. If the TyrD° signal visible at room temperature did contribute to the split EPR signal, a phase with a  $t_{1/2}$  equal to that of split EPR signal should be detected also at low microwave power. This is not the case.

Fig. 4A shows that a small contribution of  $S_2$  (less than 10% of the PS II centers) is still present after flash illumination. However, this contribution does not affect the conclusions drawn above.

If the decrease in the amplitude of the TyrD° signal recorded under non-saturating conditions and observed between times 0 and 300 s (Figs. 3B and 5A) includes a decrease in the number of spins which is associated with the loss of the split EPR signal, then the amplitude of this decay indicates that the number of centers in which it occurs is small. This proportion of centers becomes negligible when the slow phase of the TyrD° decay, which is not associated with the split EPR signal, is taken into account. The  $S_3$  state would therefore be formed in a negligible fraction of centers. This hypothesis may be ruled out, since it has been previously shown that the  $S_3$  state was formed in large majority of the centers [18].

At 0°C, we have previously found a  $t_{1/2}$  of 4.5 min for the deactivation of the split  $S_3$  signal back to  $S_2$  [15]. Therefore, the present results show that the stability of the split EPR signal is decreased at room temperature. We found no TyrD° reduction during the time required for the  $S_3$  to  $S_2$  transition at 0°C [27]. Deactivation of the  $S_2$ -state into the  $S_1$ -state required more than 48 h at 0°C for completion (not shown, but see [30]). During this long incubation, about 40 to 50% of TyrD° disappeared. The proportion of centers in which TyrD° is reduced with a  $t_{1/2}$  of 780 s can also be estimated to be 40% from the results presented in Fig. 5A.

In all the results presented above, illumination of the samples was done by flashes. The use of continuous illumination gave somewhat different results. Indeed, all the kinetics contained three or more phases, which makes their attribution difficult. In particular, in some experiments, a proportion of TyrD° decayed with a  $t_{1/2}$  varying between 200 s and 400 s. This  $t_{1/2}$  appeared nevertheless longer than that of the split EPR signal in the same conditions. The fast phase observed with a high, saturating microwave power was absent with a low, non-saturating

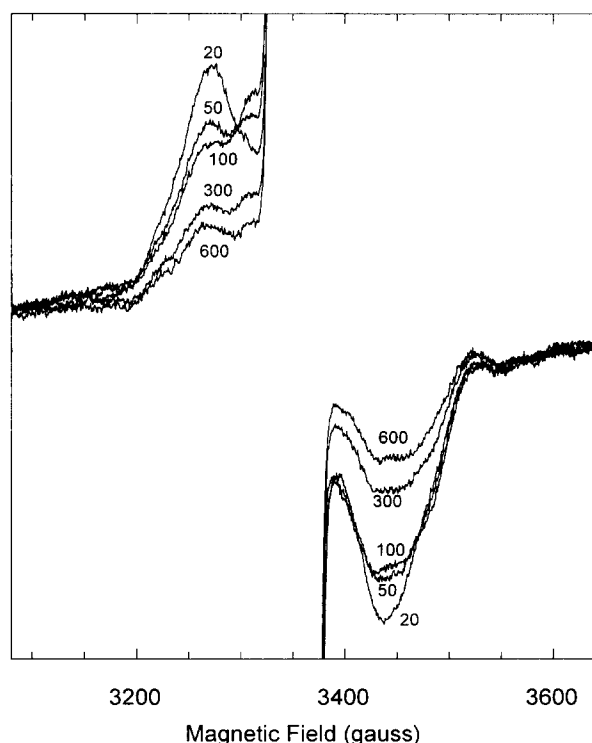


Fig. 6. EPR spectra of  $\text{Ca}^{2+}$ -depleted, EGTA-treated and polypeptide-reconstituted PS II. The spectra were recorded on a sample illuminated at room temperature by the indicated number of flashes spaced by one second and frozen after illumination. Same instrument settings as in Fig. 1 except for modulation amplitude, 15 G and microwave power, 10 mW. The central parts of the spectra corresponding to the  $\text{TyrD}^\circ$  region were deleted.

microwave power, as seen with experiments using flash illumination.

Flash illumination presents a second advantage over continuous illumination. This is illustrated in Fig. 6, which shows the effects of an increasing number of flashes on the amplitude of the split EPR signal. The number accompanying each spectrum indicates the number of flashes. Similar results were obtained with continuous illumination, which clearly results in multiple turnovers. Fig. 6 shows that over-illumination decreased the intensity of the signal by almost 70%. This decrease is accompanied by a modification of the shape. No concomitant increase of the multiline signal was observed. These effects are not due to a photoinhibitory process, since after a further dark-incubation following the illumination, the stable multiline was almost fully restored and short re-illumination again induced a split signal with a large amplitude and a normal shape (not shown). These effects of over-illumination are not understood at present. However, they are presented to demonstrate that the length of the illumination is a crucial parameter when a spin count of the split EPR signal is done.

The possibility that the split  $\text{S}_3$  EPR signal arises from a stable  $\text{TyrZ}^\circ$  is often discussed. The published experi-

mental data which are used to assign the split EPR signal to  $\text{TyrZ}^\circ$  are observations that, in samples in which the split EPR signal is observed at low temperature, a light-induced  $\text{Tyr}^\circ$  signal is also observable at room temperature. It must be assumed that the coupling which gives the splitting at low temperature is absent at room temperature. However, under the conditions used in the present work, it seems clear that when the split EPR signal is observable at helium temperature, long-lived  $\text{TyrZ}^\circ$  is not detected at room temperature. The decay of the  $\text{Tyr}^\circ$  signal recorded under saturating microwave powers which match the decay of the split EPR signal is attributed to a relaxation enhancement of  $\text{TyrD}^\circ$  by the  $\text{S}_3$  state. The slow  $\text{Tyr}^\circ$  decay recorded using non-saturating microwave powers is attributed to  $\text{TyrD}^\circ$  reduction and occurs on a time-scale significantly slower than the decay of the  $\text{S}_3$  state. Finally, the number of centers in which the split signal can be formed is sometimes reported in the literature to be low (see, for example, [31]). It is shown here that the conditions of illumination should be controlled as much as possible to obtain maximum yield of the split  $\text{S}_3$  signal.

The apparent absence of a  $\text{Tyr}^\circ$  signal at room temperature, as demonstrated here, has no bearing on the origin of the split signal. Indeed, it was the absence of the  $\text{TyrZ}^\circ$  signal at room temperature that led us to a serious consideration of  $\text{TyrZ}^\circ$  as a candidate for the split EPR signal. In a recent review, we concluded that published spectroscopic work is best explained in terms of a histidine radical rather than a tyrosine radical [22]. This is still the case at the time of writing; indeed, the recent FTIR spectrum of the  $\text{S}_2$  to  $\text{S}_3$  transition in  $\text{Ca}^{2+}$ -depleted PS II, which concludes that the spectrum is more characteristic of histidine than tyrosine radical [25], supports this proposition. Recently, however, pulsed-ENDOR data were presented by D. Britt at the ESF workshop on the oxygen-evolving enzyme (Gif sur Yvette, November 1994). These data were taken as the first spectroscopic information in favor of  $\text{Tyr}^\circ$  rather than  $\text{His}^\circ$ . We conclude, as we have done earlier, that the identity of the organic radical remains open; however, the published data clearly favor histidine over tyrosine.

## References

- [1] Michel, H. and Deisenhofer, J. (1988) *Biochemistry* 27, 1–7.
- [2] Debus, R.J., Barry, B.A., Sithole, I., Babcock, G.T. and McIntosh, L. (1988) *Biochemistry* 27, 9071–9074.
- [3] Metz, J.G., Nixon, P.J., Rogner, M., Brudvig, G.W. and Diner, B.A. (1989) *Biochemistry* 28, 6960–6969.
- [4] Barry, B.A. and Babcock, G.T. (1987) *Proc. Natl. Acad. Sci. USA* 84, 7099–7103.
- [5] Debus, R.J. (1992) *Biochim. Biophys. Acta* 1102, 269–352.
- [6] Rutherford, A.W. (1989) *Trends Biochem. Sci.* 14, 6, 227–232.
- [7] Kok, B., Forbush, B. and McGloin, M. (1970) *Photochem. Photobiol.* 11, 457–475.
- [8] Debus, R.J., Barry, B.A., Babcock, G.T. and McIntosh, L. (1988) *Proc. Natl. Acad. Sci. USA* 85, 427–430.
- [9] Vermaas, W.F.J., Rutherford, A.W. and Hansson, O. (1988) *Proc. Natl. Acad. Sci. USA* 85, 8477–8481.

- [10] Homann, P.H. (1987) *J. Bioenerg. Biomemb* 19, 105–123.
- [11] Rutherford, A.W., Zimmermann, J.-L. and Boussac, A. (1992) in *The photosystems: Structure, function and molecular biology* (Barber, J., ed.), pp. 179–229, Elsevier.
- [12] Yocum, C.F. (1991) *Biochim. Biophys. Acta* 1059, 1–15.
- [13] Boussac, A., Maisson-Peteri, B., Vernotte, C. and Etienne, A.-L. (1985) *Biochim. Biophys. Acta* 808, 231–234.
- [14] Boussac, A. and Rutherford, A.W. (1988) *Biochemistry* 27, 3476–3483.
- [15] Boussac, A., Zimmermann, J.-L. and Rutherford, A.W. (1989) *Biochemistry* 28, 8984–8989.
- [16] Boussac, A., Zimmermann, J.-L. and Rutherford, A.W. (1990) *FEBS Lett.* 277, 69–74.
- [17] Boussac, A., Zimmermann, J.-L., Rutherford, A.W., and Lavergne, J. (1990) *Nature* 347, 303–306.
- [18] Zimmermann, J.-L., Boussac, A. and Rutherford, A.W. (1993) *Biochemistry* 32, 4831–4841.
- [19] Ghanotakis, D.M., Babcock, G.T. and Yocum, C.F. (1984) *FEBS Lett.* 167, 127–130.
- [20] De Paula, J.C., Li, P., Miller, A.F., Wu, B.W. and Brudvig, G.W. (1986) *Biochemistry* 25, 6487–6494.
- [21] Boussac, A., Sétif, P. and Rutherford, A.W. (1992) *Biochemistry* 31, 1224–1234.
- [22] Rutherford, A.W. and Boussac, A. (1992) in *Research in Photosynthesis* (Murata, N., ed.), Vol. II, pp. 21–27, Kluwer, Dordrecht.
- [23] Boussac, A. and Rutherford, A.W. (1994) *Biochem. Soc. Trans.* 22, 352–358.
- [24] Hogansson, C.W. and Babcock, G.T. (1994) in *Metals Ions in Biological Systems* (Sigel, H. and Sigel, A., eds.), Vol. 30, pp. 77–107, Marcel Dekker, New York.
- [25] Berthomieu, C. and Boussac, A. (1995) *Biochemistry* 34, 1541–1548.
- [26] Hallahan, B.J., Nugent, J.H.A., Warden, J.T. and Evans, M.C.W. (1992) *Biochemistry* 31, 4562–4573.
- [27] Boussac, A. and Rutherford, A.W. (1992) *Biochemistry* 31, 7441–7445.
- [28] Deak, Z., Vass, I. and Styring, S. (1994) *Biochim. Biophys. Acta* 1185, 65–74.
- [29] Sivaraja, M., Tso, J. and Dismukes, G.C. (1989) *Biochemistry* 28, 9459–9464.
- [30] Ono, T.-A. and Inoue, Y. (1989) *Biochim. Biophys. Acta* 973, 443–449.
- [31] Gilchrist, M.L., Lorigan, G.A. and Britt, R.D. (1992) in *Research in Photosynthesis* (Murata, N., ed.), Vol. II, pp. 317–320, Kluwer, Dordrecht.